Electronic Supplementary Material (ESI) for Chemical Communications
This journal is © The Royal Society of Chemistry 2012

Electronic Supplementary Information (ESI) for Chemical Communications
This journal is © The Royal Society of Chemistry 2012

Supplementary Information

Sub-oxide-to-metallic, uniformly-nanoporous crystalline nanowires by plasma oxidation and electron reduction

Uroš Cvelbar[*,a], Zhiqiang Chen[b], Igor Levchenko[c,d], R. Michael Sheetz[e], Jacek B. Jasinski[d], Madhu Menon[e,f], Mahendra K. Sunkara[b] and Kostya (Ken) Ostrikov[c,d]

[a]*Jozef Stefan Institute, Jamova cesta 39, Ljubljana, SI 1000, EU*

[b]*CONN Centre for Renewable Research, University of Louisville, Louisville, KY 40292, USA*

[c]*Plasma Nanoscience Centre Australia (PNCA), CSIRO Materials Science and Engineering, P.O.Box 218, Lindfield, NSW 2070, Australia*

[d]*Plasma Nanoscience, School of Physics, The University of Sydney, Sydney, NSW 2006, Australia*

[e]*Center for Computational Sciences, University of Kentucky, Lexington, KY 40506-0045, USA*

[f]*Department of Physics and Astronomy, University of Kentucky, Lexington, KY 40506-0055, USA*

Table of Contents

Electronic Supplementary Information (ESI) for Chemical Communications
This journal is © The Royal Society of Chemistry 2012

1. Details of nanowire synthesis

The single crystal molybdenum oxide nanowires are synthesised via RF-PECVD method. The pure Mo foil (99.99% Alfa Aeser) is exposed to RF plasma created in oxygen gas discharge with the density of neutral oxygen atoms $1.2 \cdot 10^{21}$ m^{-3} , and the density of charge species is 10^{15} m^{-3} with the average energy of 2 eV. The plasma is created in a vacuum reactor with the base pressure of 1 Pa. During the creation of oxide layer on Mo foil and increase of its surface temperature, molybdenum oxide tends to evaporate from the sample. The evaporated oxide is deposited to 20 mm distant borosilicate glass plate or even SS plate, heated to approx. 500^{o}C. Due to interaction of evaporated molybdenum oxide and interaction with oxygen plasma radicals, localized Mo-O plasma is created between the Mo foil and deposition plate. With this plasma, MoO_3 nanowires are synthesised and deposited on the substrate holder surface in dense arrays. The length of grown NWs grown in array (as seen from images below) is 1-2 μm with diameter of 40 – 80 nm. A typical length-to-diameter ratio is 20. The growth of NWs and their morpholology depends strongly on plasma parameters which are typically controlled by discharge parameters (e.g. discharge input power, gas flow rate, partial pressure in reactor chamber, etc.) as well as on the sample substrate temperature.

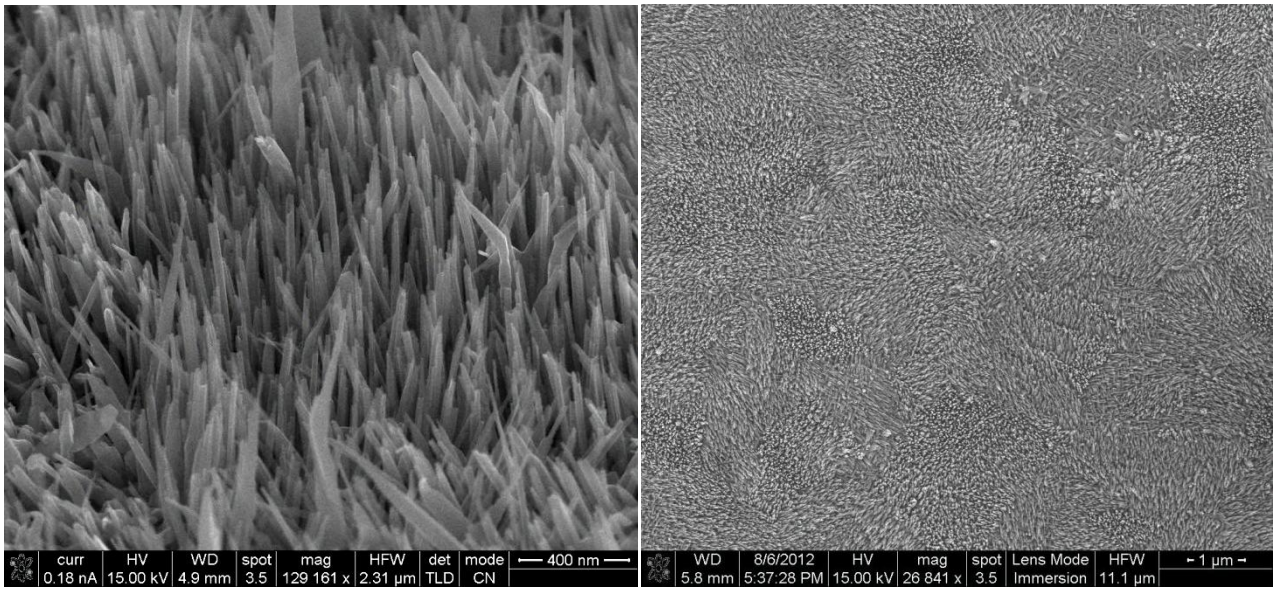

Fig. S1. The FE-SEM images showing arrays of MoO_3 NW deposited on the substrate.

Electronic Supplementary Information (ESI) for Chemical Communications
This journal is © The Royal Society of Chemistry 2012

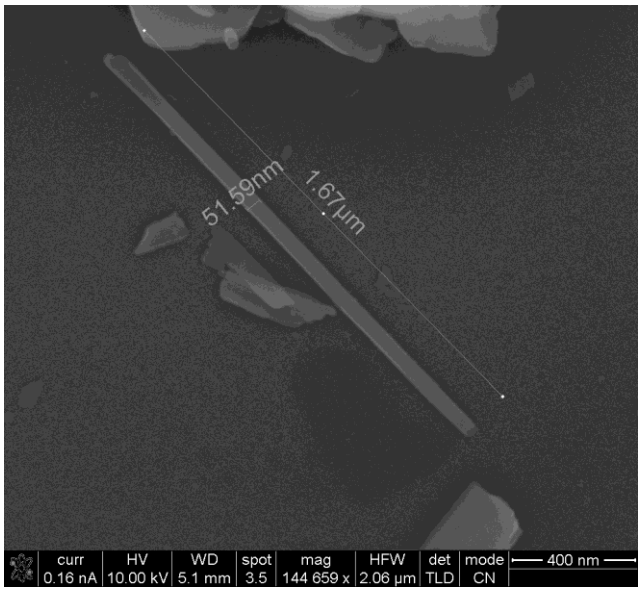

Fig. S2. The MoO_3 NW characteristic dimension analyzed when NWs were scratched from the substrate.

2. Electron beam irradiation and sample analysis

The in-situ studies were carried out using 200kV inside a TECNAI F20 TEM. Selected nanowire was illuminated with a beam current of 9.78 nA. The pressure in the microscope was ~10^{-10} torr. Images were recorded at every 2 minutes with a CCD camera with a cold trapper so that contamination was minimized. Selected area diffraction patterns are recorded on the other nanowire at every 10 min. EELS are recorded at TEM diffraction mode at 0.1eV/channel. The spectra was aligned and fitted with the first spectrum by MLS fitting method in Digitalmicrograph software (Gatan Inc.).

XRD measurements were conducted using a Burker Discovery D8 diffractometer with a non-monochromated X-ray beam of Cu Kα radiation (0.154 nm). XRD spectra were analyzed with Bruker EVA software and the PDF-2 Database from International Center for Diffraction Data was used for crystallographic phase searching and identification. The results are shown in Fig S3. For the X-ray photoelectron spectroscopy (XPS) analyses we used PHI-TFA XPS spectrometer produced by Physical Electronics Inc. The analyzed area was 0.4 mm in diameter and the analyzed depth was about 5 nm. Sample surfaces were excited by X-ray radiation from Al monochromatic source at photon energy of 1486.6 eV. The survey spectra were acquired over wide energy range to identify and quantify the elements. The accuracy of binding energy was about 0.3 eV. The results of MoO_3 phase are shown in Fig S4.

Electronic Supplementary Information (ESI) for Chemical Communications
This journal is © The Royal Society of Chemistry 2012

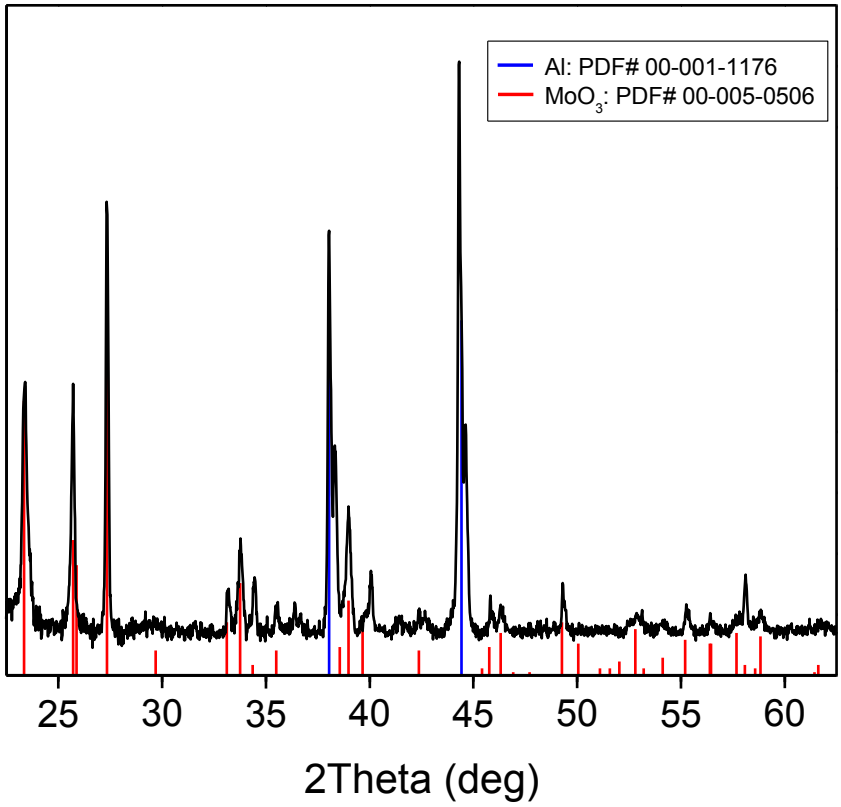

Fig. S3. XRD spectra of MoO_3 NWs on polycrystalline aluminium substrate with marked peaks from Powder Diffraction Files.

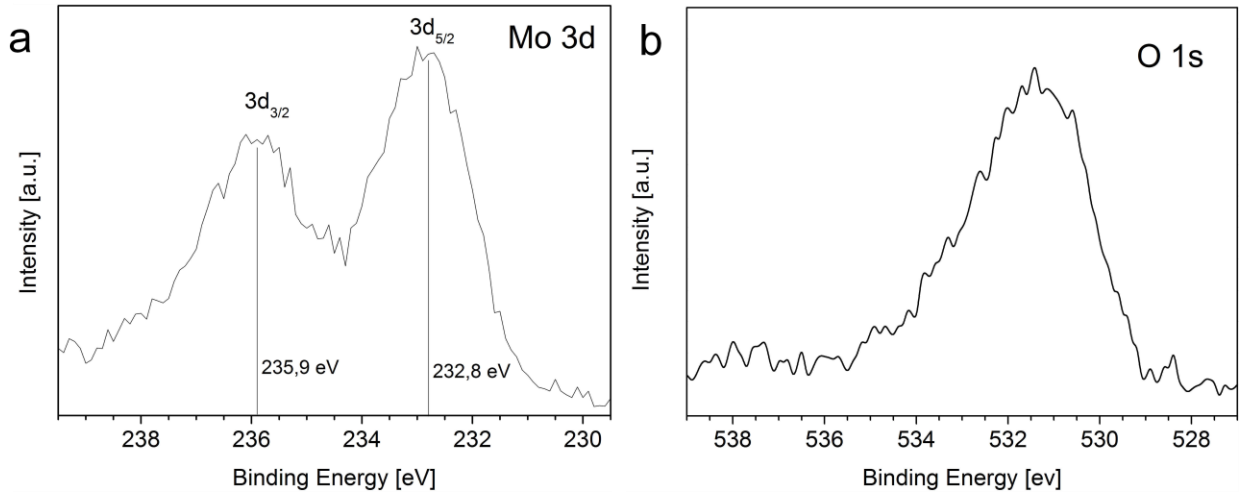

Fig. S4. The XPS spectra of MoO_3 with characteristic (a) doublet peak of Mo 3d presenting hexavalent molybdenum at 235.9 eV and 232.8 eV, which corresponds to Mo $3d_{3/2}$ and Mo $3d_{5/2}$ orbitals, respectively [C.D. Wagner et al (Eds.) Handbook of XPS, 1979, USA] and (b) O 1s peak. The calculated Mo/O ratio for the sample analyzed was 1/3.

Electronic Supplementary Information (ESI) for Chemical Communications
This journal is © The Royal Society of Chemistry 2012

3. Evolution of pores in MoO_3 nanowire (movie)

File MoO3_Porosity.wmv shows a movie of the evolution of pores in the MoO_3 nanowire through bright-field images with continuous exposure to electron beam radiation.

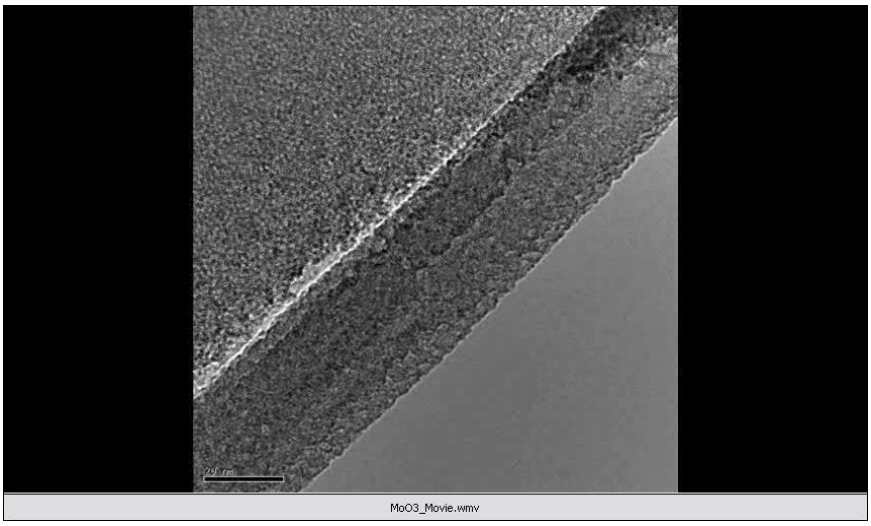

Fig. S5. Snapshot from MoO3_Movie.wmv file showing of pores within MoO_3 nanowire.

4. Fabrication of nanoporous $W_{18}O_{49}$ nanowires

Tungsten oxide nanowires were synthesized using chemical vapour transport of tungsten oxide vapours with air flow (11 sccm air, 0.770 Torr pressure) over hot-filaments kept at 1900 C on to quartz substrates kept at about 550 C or lower. The as-synthesized nanowires were scrapped from the quartz substrate and were transferred to TEM grid. The same parameters used for irradiation of MoO_3 NW were used for irradiation of WO_3 NW for about 2 hours.

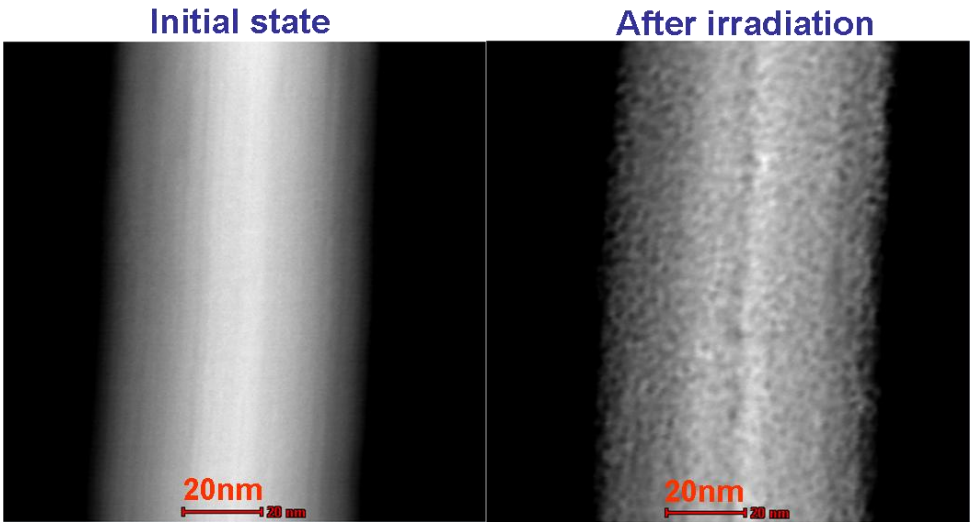

Fig. S6. Bright field image of tungsten oxide nanowires before and after electron beam irradiation for 2 hours.

Electronic Supplementary Information (ESI) for Chemical Communications
This journal is © The Royal Society of Chemistry 2012

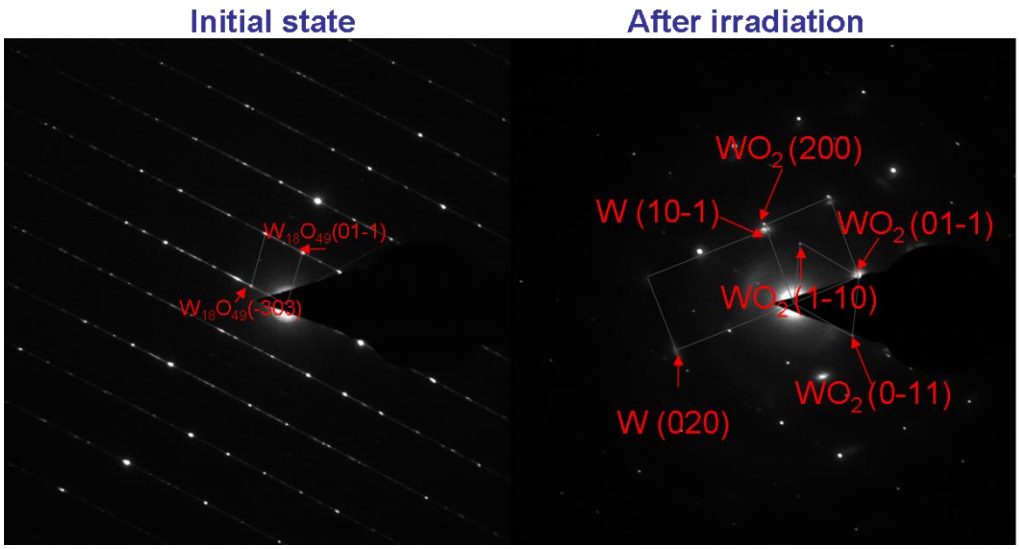

Fig. S7. The diffraction patterns of tungsten oxide nanowires before and after electron beam irradiation. The as-synthesized tungsten oxide nanowires were of $W_{18}O_{49}$ phase with randomly ordered oxygen vacancy planes. After irradiation, the porous nanowires exhibited both tungsten and reduced WO_2 phases together.

5. Estimation of nanowire composition

Let us consider the mass reduction of the nanowire during EBI, and compare the expected porosity with the numbers calculated directly from the TEM images.

The porosity coefficient ($0 < \chi < 1$) can be written in the form: $\chi = \frac{V_{void}}{V_0}$;

where V_{void} is the volume of voids (holes), and V_0 is the volume of the whole nanowire.

Hence, for the MoO_3 → MoO_2 transformation: $\chi = \frac{V_{void}}{V_0} = \frac{V_0 - V_{MoO_2}}{V_0} = 1 - \frac{V_{MoO_2}}{V_0} = 1 - k\frac{\rho_{MoO_3}}{\rho_{MoO_2}}$,

where k is the mass reduction coefficient, ρ_{MoO_3} is mass density of MoO_3, and ρ_{MoO_2} is mass density of MoO_2.

Thus, the porosity coefficient can be found as $\chi = 1 - k\frac{\rho_{MoO_3}}{\rho_{MoO_2}}$. Using mass density numbers for of MoO_3 and MoO_2 (4.69 and 6.47 g×cm^{-3}) and mass reduction coefficient $k=0.89$ (for the case of one O atom removal), we obtain the expected porosity coefficient $\chi=0.35$.

Similar calculations for the MoO_3 → Mo transformation give the expected porosity coefficient $\chi=0.69$.

Electronic Supplementary Information (ESI) for Chemical Communications
This journal is © The Royal Society of Chemistry 2012

Geometrical analysis of the TEM image of the porous nanowire gives the porosity coefficient χ can be up to 0.5. Thus we can conclude that, given that the electron beam irradiation preferentially removes oxygen atoms (O atom mass is 16 versus 96 for Mo, this means that the probability of Mo atom removal by the electron impact is much lower than the probability of O removal), the resultant porous nanowires may consist even of pure molybdenum.

Assuming that complete removal of oxygen is questionable, we can conclude that the porous nanowires are MoO_X, with X tending to zero.

6. DFT computations of the formation of localized metallic clusters

A general mechanism for O^+ desorption from transition metal oxides and, in particular, from TiO_2 has been proposed by Knotek and Feibelman.[1] A refined version of this mechanism by taking into account the high degree of covalency in transition metal oxides has also been proposed recently.[2] We investigate the subsequent desorption of O atoms in MoO_3 nanowires leading to the pore formation by carrying out theoretical simulations using the Density Functional Theory (DFT) computations as implemented in the CASTEP program[3] on a 3×1×3 nanowire segment subject to periodic boundary conditions. The fully optimized structure is shown in Fig. S8. The O desorption from nanowires bulk is simulated by removing one of the oxygen atoms between the double layers of linked MoO_6 octahedra (shown in white in Fig. S8, left) and optimizing the geometry. This oxygen atom was selected for initial desorption since these oxygens, located at the interface of successive double layers that interact only via van der Waals forces, would be more weakly bound than oxygens within the plane of the double layer that are bound to two Mo atoms.

The optimized nanowire structure (MoO_3-1O) shows local distortions (Fig. S8, middle). Our computations show a redistribution of charge within the nanowire upon desorption of a single oxygen atom. While a number of oxygens near the site of O desorption exhibited an accumulation of negative charge, a number of oxygens exhibited a measurable increase in positive charge. In particular, one of the O atom near the O desorption site exhibited a dramatic increase in positive charge of more than 25% (shown in white in Fig. S8, middle). Such a significant increase in positive charge might be expected to destabilize the Mo-O bonding between this oxygen and its two nearest-neighbour Mo atoms due to an increase in Coulomb repulsion by the positively charged Mo atoms in the nanowire lattice. Indeed, our calculations do show a measurable increase in the bond length (16%) between this atom and the Mo

Electronic Supplementary Information (ESI) for Chemical Communications
This journal is © The Royal Society of Chemistry 2012

from which O desorption occurs as well as a decrease in the electron density within this bond, both indicating that this oxygen becomes much more weakly bound following desorption of the initial O atom. Detailed electronic structure analysis point to the hybridization of a *p*-orbital electron with a localized hole on an adjacent Mo atom to be responsible for the increase in positive charge on an O atom adjacent to the site of O desorption. Our calculations do show a decrease in the electron density within the *p*-orbital of the oxygen exhibiting this increase in positive charge. Moreover, the adjacent Mo from which the initial O atom was removed also shows an increase in positive charge (relative to the other Mo atoms in the nanowire), a significant decrease in electron density within its *p*-orbital, and an increase in electron density within its *d*-orbital. The electronic structure calculations show development of metallicity on the desorption of a single O atom in MoO_3 which is a wide band-gap semiconductor prior to desorption. We carried out our study further by investigating the effects of the desorption of the second O atom following the desorption of the first O atom. The second O atom that was removed was the oxygen (white atom in Fig. 8b, middle) exhibiting the greatest increase in positive charge and largest increase in Mo-O bond length and, therefore, the weakest bonding following the initial desorption event. The optimized geometry of the resulting MoO_3-2O structure (original MoO_3 nanowire with two desorbed oxygens) is shown in Fig. S8, right. The charge distribution within the MoO_3-2O nanowire is found to be completely different than that for the MoO_3-1O nanowire. In particular, we see that three of the four oxygen atoms bonded to the Mo atom from which the first O atom was desorbed show a small but measurable increase in positive charge along with a small reduction in *p*-orbital electron density in contrast to the same atoms in MoO_3-1O which showed either no change in charge or a slight increase in negative charge. The metallic conductivity of MoO_3-2O also exhibited a significant increase.

Our calculations, thus, point to a phase transformation of MoO_3 via the occurrence of a localized structural change induced by desorption of multiple oxygen atoms at particular sites within the nanowire. As shown by us, the desorption of one O^+ increases the susceptibility of neighboring oxygen atoms to be desorbed due to the latter gaining an increased positive charge relative to non-neighbor oxygen atoms. This increased positive charge would result in an increase in Coulomb repulsion by the surrounding positively charged Mo atoms making these O atoms more likely to undergo desorption from the nanowire. The hybridization of an electron from an O atom with a hole on the Mo atom at the site of the initial O desorption (responsible for the increase in positive charge on the oxygen atom) can be greatly facilitated by a reduction in the rate of electron-hole pair recombination on the Mo atom, thereby increasing the lifetime of the hole on the Mo atom. The occurrence of metallicity in the MoO_3

Electronic Supplementary Information (ESI) for Chemical Communications
This journal is © The Royal Society of Chemistry 2012

nanowire found by us upon desorption of an O atom lends strong support to this. This permits the electron from an electron-hole pair to be easily transferred from the valence to the conduction band. The subsequent delocalization of the electron across the nanowire would result in the separation of the electron-hole pair, leaving the hole on the Mo atom to hybridize with an electron in the p-orbital of an adjacent O atom. One of the most interesting results of these calculations is that, following desorption of two oxygen atoms, the optimized nanowire geometry shows the formation of a ziz-zag pore (shown in green in Fig. S8, right) localized at the site of desorption of the two O atoms. These results suggest that the formation of pores in a MoO_3 nanowire following electron beam irradiation is due to a conformation change (phase transformation) within the nanowire subsequent to the radiation-induced desorption of multiple oxygen atoms from within the bulk of the nanowire.

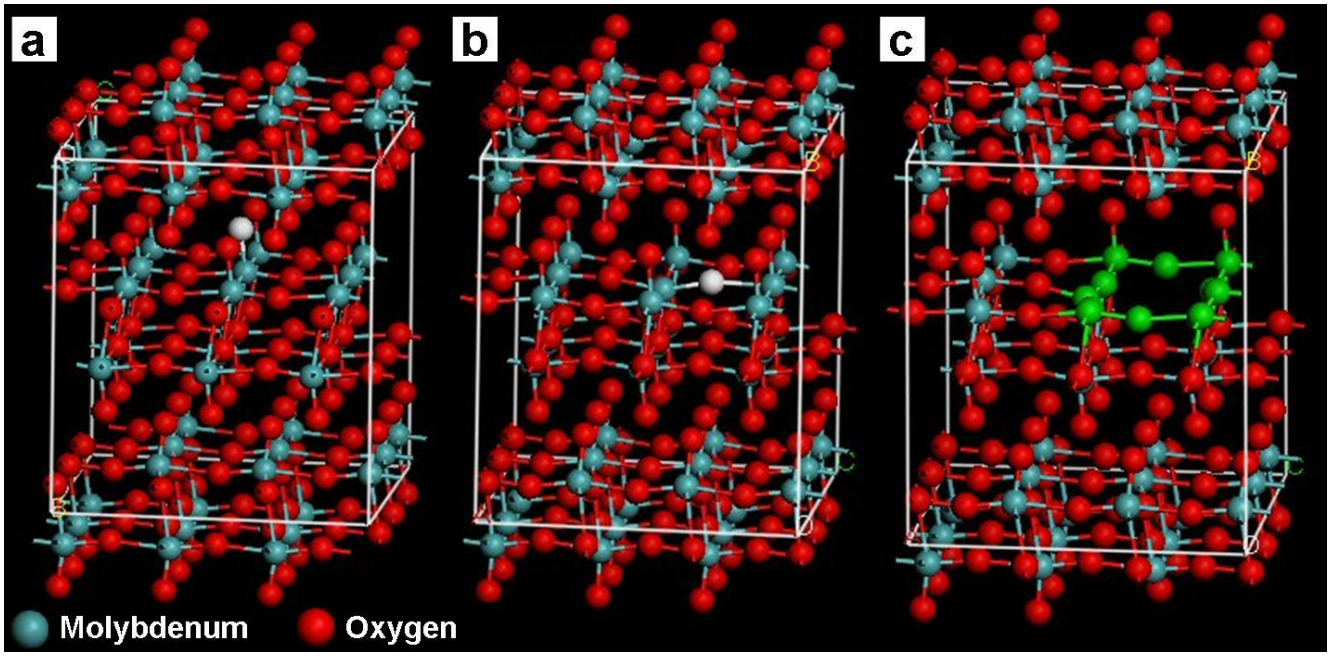

Fig. S8. Optimized 3×1×3 MoO_3 nanowire segment (left). The middle and right panels show, respectively, optimized (b) MoO_3-1O and (c) MoO_3-2O nanowire segments.

1 M. L. Knotek and P. J. Feibelman, *Phy. Rev. Lett.*, 1978, **40**, 964.

2 S. I. Tanaka, K. Mase, and S. I. Nagaoka, *Surf. Sci.*, 2004, **572**, 43.

3 M. D. Segall, P. J. D. Lindan, M. F. Probert, C. J. Pickard, P. F. Hasnip, S. J. Clark and M. C. Payne, *J. Phys.: Condens. Matter.*, 2002, **14**, 2717.